Electronic structure of random $Al_{0.5}Ga_{0.5}As$ alloys: Test of the "special-quasirandom-structures" description

K. C. Hass and L. C. Davis
Research Staff, Ford Motor Company, Dearborn, Michigan 48121-2053

Alex Zunger
Solar Energy Research Institute, Golden, Colorado 80401
(Received 21 May 1990)

The spectral properties of an sp^3s^* tight-binding Hamiltonian for a random, unrelaxed $Al_{0.5}Ga_{0.5}As$ alloy are calculated using three different techniques: the coherent-potential approximation, the recursion method (as applied to a > 2000 atom supercell), and the recently introduced "special-quasirandom-structures" (SQS) approach. Over a broad range of scattering strengths, the dominant spectral features predicted by the first two techniques are well reproduced by calculations for an SQS with 16 atoms/unit-cell ("SQS-8"). This suggests that the SQS approach might also be useful in cases where the other methods are difficult to apply, e.g., in first-principles calculations for structurally relaxed alloys.

A great deal of progress has been made in the last few decades in understanding the effects of disorder in random alloys. Much insight into this problem has been obtained by applying effective medium techniques—e.g., the coherent-potential approximation[1] (CPA)—to model Hamiltonians with varying degrees of realism. While some success has also been achieved in implementing the CPA in first-principles band-structure formalisms,[2] this approach is extremely costly and has not yet addressed the problem of structural relaxation. Deviations from an ideal lattice structure are particularly important in semiconductor alloys where individual atoms are often displaced *locally* (due to strong bond-stretching forces) even though Vegard's law may be obeyed on average.[3]

An alternative approach to calculating the electronic structure of a random $A_{1-x}B_x$ substitutional alloy is to consider a large supercell with N lattice sites occupied randomly by A and B atoms.[4] Unlike the CPA, which is a single-site theory, the supercell approach also includes the effects of the local chemical (and, in a structurally relaxed alloy, positional) environments about each site. This approach becomes exact in the limit of large N. In practice, however, this limit of a perfectly random alloy is approached only slowly and irregularly. Calculations for sufficiently large supercells ($N > 500$) are therefore intractable using first-principles techniques; studies of such large-N structures have therefore been limited to model Hamiltonians and have required specialized techniques such as the recursion method.[5]

Recently, Zunger and co-workers[6,7] have introduced an approach that greatly reduces the size of the supercell required to obtain a realistic description of a random alloy. Instead of occupying the supercell sites at random, these authors optimize the arrangement of the A and B atoms, for a given N, so that the structure as a whole mimics the lowest-order correlation functions (pair and many-body) of an infinite random alloy. In the case of fcc symmetry, even for $N = 8$, the resulting "special quasirandom structure" (SQS-8) already reproduces exactly the pair corre-

lation functions for the first two fcc coordination shells and introduces only modest errors in subsequent shells. For an $A_{0.5}B_{0.5}C$ zinc-blende (ZB) -structure pseudobinary alloy, SQS-8 is a superlattice having an $A_2B_3A_2B_1$ cation ordering along the [113] direction and 16 atoms/unit-cell.[8] Such a small-period structure is easily handled using first-principles techniques, including the effects of charge transfer and structural relaxation. Early uses of this approach for modeling the thermodynamic properties and band-gap bowing in a wide range of ZB pseudobinary alloys have been extremely promising.[6,7]

In view of the potential importance of the SQS concept, it is useful to test this approach against more conventional theories of random alloys under conditions where the latter are known to work well. As an initial step in this direction, we present in this paper a comparison of electronic structure results obtained using (i) the CPA, (ii) the recursion method applied to a randomly occupied supercell with $N > 2000$, and (iii) SQS-8, all for the same model Hamiltonian. In each case, we assume an unrelaxed alloy described by an sp^3s^* tight-binding Hamiltonian[9] nominally representative of $Al_{0.5}Ga_{0.5}As$. We focus primarily on the case of cation site-diagonal disorder, which both the CPA and the recursion methods are known to treat well; this approximation and the neglect of structural relaxation are believed to be reasonable in $Al_xGa_{1-x}As$ because of the excellent lattice match between AlAs and GaAs.

Specifically, we consider a tight-binding Hamiltonian for $Al_{0.5}Ga_{0.5}As$ of the form

$$H = H_{VCA} + \lambda \Delta V_c . \tag{1}$$

The first term is a periodic, virtual-crystal approximation (VCA) contribution obtained by averaging the AlAs and GaAs parameters of Ref. 9 after subtracting 0.47 eV from the AlAs diagonal parameters to provide an intrinsic band offset.[10] The second term describes the deviations from the VCA diagonal parameters at cation sites; λ is a scaling

parameter that allows us to vary the differences between Al and Ga diagonal parameters from zero (VCA) to that of the crystalline parametrizations ($\lambda = 1$) and beyond. Since we are primarily interested in a comparison of different theoretical predictions, we will not concern ourselves with the question of how accurately the present model describes $Al_{0.5}Ga_{0.5}As$. It is sufficient for our purposes that Eq. (1) provides reasonable valence and lower conduction bands and a range of scattering strengths.[11] (For $\lambda = 1$, the Ga s, p, and s^* levels differ from those of Al by -1.02, $+0.55$, and $+0.48$ eV, respectively.) For reference, we list in the first two columns in Table I the Γ_1, X_1, and X_3 conduction-band eigenvalues obtained by replacing the cation diagonal parameters in H_{VCA} by their values in GaAs and AlAs, respectively.[12] The absolute VCA energies associated with these states are given in the third column. As we will see, the scattering strengths associated with these three states cover the entire range usually encountered in semiconductor alloys.

The electronic structure in a random $Al_{0.5}Ga_{0.5}As$ alloy is conveniently discussed in terms of the spectral function $A(\mathbf{k},E)$, which represents the probability of finding an electron with zinc-blende-structure wave vector $\mathbf{k}$ and energy E. In a real alloy, as well as in the CPA and recursion methods, $A(\mathbf{k},E)$ is a continuous function whose shape is determined by the strength of disorder-induced scattering at different energies. In a small-N periodic structure, such as an SQS, on the other hand, $A(\mathbf{k},E)$ reduces to a sum of δ functions. Indeed, the electronic structure of an SQS may be described in terms of Bloch states $|n,\mathbf{K}\rangle$ with energies $E_{n\mathbf{K}}$ and SQS wave vectors $\mathbf{K}$. Because the SQS Brillouin zone is smaller than its ZB counterpart, a given ZB Bloch state $|a,\mathbf{k}\rangle$ projects onto a range of SQS states of compatible symmetry. The SQS spectral function may then be written as

$$A(\mathbf{k},E) = \sum_a \sum_T \sum_{n,\mathbf{K}} N_T^{-1} |\langle a,\underline{T}\mathbf{k} | n,\mathbf{K}\rangle|^2 \delta(E - E_{n\mathbf{K}}), \quad (2)$$

where the first sum is over a complete set of states and $\underline{T}$ ranges over all N_T symmetry operations of the ZB-structure point group.[13] Given the discreteness of $A(\mathbf{k},E)$ for a small-N periodic structure, it is also useful to examine the integrated spectral moments

$$M_p(\mathbf{k}) = \int_{E_1}^{E_2} dE\, E^p A(\mathbf{k},E), \quad (3)$$

where p is an integer. Of particular interest here[14] will be the "widths" of various spectral features, characterized by the difference $\mu_2(\mathbf{k}) = M_2(\mathbf{k}) - [M_1(\mathbf{k})]^2$.

CPA spectral functions for the present model are computed using standard techniques.[15] The recursion method is implemented using randomly generated clusters of 2048–2304 atoms, with periodic boundary conditions, and 200 levels of recursion.[4] The recursion results do not depend significantly on the particular cluster realization and, of the three methods discussed here, are believed to be most representative of the exact spectral properties of the random alloy. Peak positions in the calculated theoretical spectra for $Al_{0.5}Ga_{0.5}As$ are listed in Table I.

Figure 1 compares the calculated SQS-8 spectral function at Γ ($\mathbf{k} = 0$) for $\lambda = 1$ with the corresponding CPA and recursion results. We note, first of all, that the latter
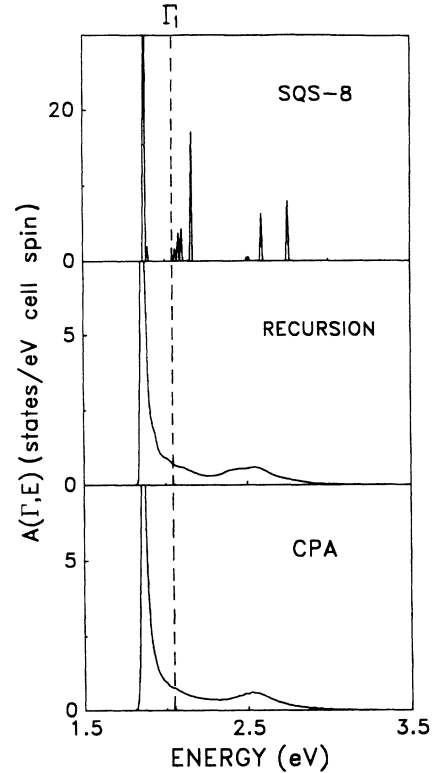

FIG. 1. Comparison of the SQS-8 spectral function at the Γ point of the zinc-blende Brillouin zone for $\lambda = 1$ with the corresponding CPA and recursion method results. The SQS-8 spectrum is actually a series of δ functions which are broadened here by 0.005 eV to ease visualization. The vertical dashed line represents the energy of the VCA Γ_1 state.

two curves are virtually indistinguishable, which we believe confirms their suitability as a standard for comparison. (See, however, Fig. 3 below.) The shape of these curves is typical of what is often obtained in semiconductor alloys:[4,15] The sharp peak at 1.86 eV is a shifted and broadened version of the VCA Γ_1 state at 2.06 eV and the additional structure near 2.5 eV results from a disorder-induced mixing of VCA states from other $\mathbf{k}$ points. (The disorder-induced shift of the lower peak is the dominant contribution to the "bowing" of the direct band gap in this system.) Both of these features are also reproduced to a large extent in the SQS-8 spectral function. The lowest SQS-8 peak occurs only 0.02 eV above that of the other two methods and the remaining SQS-8 peaks also occur at energies where the random alloy has significant spectral weight.

Because of the sensitivity of the heights of the $A(\mathbf{k},E)$ peaks in the different methods to the numerical procedures employed, the intensities of various spectral features are more meaningfully compared by integrating the results in Fig. 1 from 1.5 eV up to a higher energy cutoff [$p = 0$ in Eq. (3)]. The dashed curve labeled "random" in Fig. 2 is thereby obtained for both the recursion method and the CPA. The striking difference between this curve and the single step function predicted in the VCA results from the ΔV_c term in Eq. (1). In the traditional language of alloy theory,[1] such behavior is typical

TABLE I. Top: Location of spectral features (in eV) associated with the zinc-blende Γ_1, X_1, and X_3 states. The first two columns are obtained by replacing the cation diagonal parameters in the VCA Hamiltonian by their GaAs and AlAs values, respectively. Entries for $Al_{0.5}Ga_{0.5}As$ refer to peak positions in the appropriate spectral function for $\lambda = 1$. The final column characterizes the scattering strength associated with each state. Bottom: Calculated "widths" [defined in text; in $(eV)^2$] of Γ and X spectra shown in Figs. 1 and 3, respectively.

	"GaAs"	"AlAs"	VCA	$Al_{0.5}Ga_{0.5}As$			
				SQS-8	Recursion	CPA	
Γ_1	1.700	2.426	2.059	1.88	1.86	1.86	intermediate
X_1	2.081	1.784	1.934	1.91	1.89	1.89	weak
X_3	2.153	2.408	2.278	2.18[a]	2.21[a]	2.12[a]	strong
$\mu_2(\Gamma)$				0.079	0.077	0.078	
$\mu_2(X)$				0.045	0.048	0.060	

[a]Most intense peak associated with X_3.

of moderately strong scattering. It is thus nontrivial that the irregular staircase structure for SQS-8 in Fig. 2 provides an excellent approximation to the random-alloy result. Most importantly, SQS-8 correctly distributes the total weight over a roughly 0.8-eV region and places only a little more than half in the dominant low-energy peak. The calculated width $\mu_2(\Gamma)$ for SQS-8, obtained by integrating in Eq. (3) over the entire range in Fig. 1, is the same as that of the CPA and recursion methods to within better than 2% (cf. Table I).

A similar comparison of CPA, recursion and SQS-8 spectral functions at the X point of the ZB-structure Brillouin zone for $\lambda = 1$ is shown in Fig. 3. Here the CPA and recursion results do not agree as well as at Γ, although they are qualitatively similar. The lowest peak at 1.89 eV in the CPA and recursion results is a remnant of the VCA X_1 state and the higher energy structure is associated with X_3. The 0.04-eV downshift (cf. Table I) and broadening of the X_1 state relative to the VCA is consistent with relatively weak scattering. By contrast, the X_3 state is much

more strongly scattered, as evidenced by its nearly "split-band" behavior.[16] The greater sensitivity of the X_3 state to disorder results from the higher density of states available for scattering in the vicinity of the X_3 point and from the fact that this state has a large cation s component, which is particularly sensitive to the disorder;[17] the cation s component in the VCA X_1 state is zero, by symmetry. We believe that the discrepancy between the CPA and the recursion results in Fig. 3 is a real effect that may indicate a deficiency of the CPA in the strong scattering X_3 region.

The vastly different behaviors in the X_1 and X_3 regions are both well described by the SQS-8 results in Fig. 3. The SQS-8 spectral weight associated with X_1 is con-
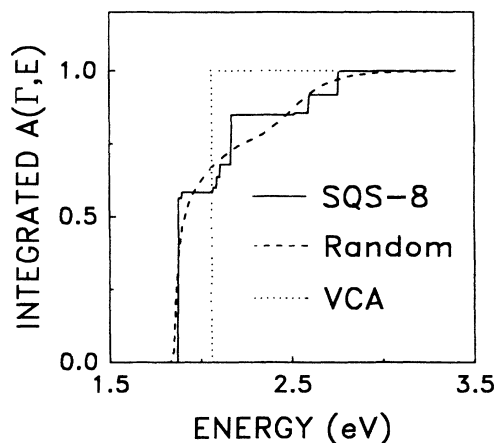

FIG. 2. Integral of the spectral function at Γ from 1.5 eV up to an energy E, vs E, for the SQS-8 results in Fig. 1 (solid), the VCA (dotted), and a random alloy (dashed). The random-alloy result is the same for both the CPA and recursion methods. The integral is normalized to give one state per cell per spin over the interval shown.
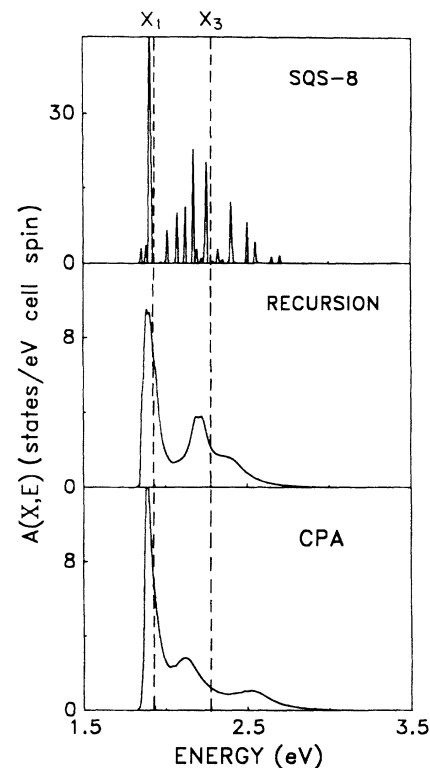

FIG. 3. Same as Fig. 1 but for the X point of the zinc-blende Brillouin zone. The vertical dashed lines represent the energies of the VCA X_1 and X_3 states.

tained almost entirely in a single peak 0.02 eV above that of the CPA and recursion methods. The principal SQS-8 X_3 peak lies 0.03 eV below the recursion prediction, which is 0.06 eV closer than the corresponding CPA peak (cf. Table I). As a function of λ, we find that the X_3 structure in all three methods begins as a single dominant peak which broadens and splits into two distinct features. The rate of splitting increases in the series recursion→ SQS-8 → CPA, at least up to $\lambda = 1.5$, with the lower of the two SQS-8 peaks remaining particularly close to the lower recursion peak throughout. The calculated widths $\mu_2(X)$ in Table I, obtained by integrating the total $A(X,E)$ spectra (i.e., including both the X_1 and X_3 regions) over the entire range of Fig. 3, differ by only 6% for the SQS-8 and recursion methods. The CPA width, by contrast, is 25% larger than the recursion result.

Even at **k** points of lower symmetry, we find that the agreement between the SQS-8 and recursion results is comparable to that in Figs. 1 and 3. This is particularly significant, indicating that although an SQS is optimized only in a statistical sense, it does well for individual **k**-resolved spectra, as well as for quantities that depend on averages over the Brillouin zone (e.g., total energies[6,7]). A related issue that we have only partially addressed is that of uniqueness. Results obtained for an $N = 8$ supercell with an Al_4Ga_4 [113] cation ordering (not an SQS) suggest that, while alternative cation distributions will

often yield results comparable to those of the "best" SQS-8 structure at *particular* **k** points, elsewhere the agreement is much worse.

The above tests demonstrate that, for the case of diagonal disorder, calculations for SQS-8 reproduce the dominant spectral features in the random alloy to within the accuracy with which these are known (characterized here by the differences between the CPA and recursion results) over a broad range of scattering strengths. Similar agreement between the SQS-8 and recursion predictions is also obtained if we do not average the nearest-neighbor tight-binding parameters as in the VCA, but instead allow the Al-As and Ga-As parameters in $Al_{0.5}Ga_{0.5}As$ to retain their crystalline values.[16] This consideration of off-diagonal disorder, which will be explored in more detail elsewhere,[18] suggests that SQS-8 should also work well for more realistic (e.g., first-principles) Hamiltonians[6] and for structurally relaxed systems, where alternative theories are difficult to implement. Unlike the CPA and recursion methods, which we have used for reference, the SQS concept is ideally suited for these cases. We thus expect that the SQS approach will prove to be a valuable complement to more traditional alloy theories.

[1]H. Ehrenreich and L. M. Schwartz, in *Solid State Physics,* edited by H. Ehrenreich, F. Seitz, and D. Turnbull (Academic, New York, 1976), Vol. 31, p. 149.

[2]H. Winter and G. M. Stocks, Phys. Rev. B **27**, 882 (1983).

[3]J. C. Mikkelsen, Jr., and J. B. Boyce, Phys. Rev. B **28**, 7130 (1983).

[4]L. C. Davis, Phys. Rev. B **28**, 6961 (1983); Mater. Sci. Forum **4**, 197 (1985).

[5]R. Haydock, in *Solid State Physics,* edited by H. Ehrenreich, F. Seitz, and D. Turnbull (Academic, New York, 1980), Vol. 35, p. 215.

[6]A. Zunger, S.-H. Wei, L. G. Ferreira, and J. E. Bernard, Phys. Rev. Lett. **65**, 353 (1990); S.-H. Wei, L. G. Ferreira, J. E. Bernard, and A. Zunger, Phys. Rev. B (to be published).

[7]S.-H. Wei and A. Zunger, Appl. Phys. Lett. **56**, 662 (1990).

[8]Interchanging A and B gives a $B_2A_3B_2A_1$ cation ordering whose spectra will be slightly different due to the reverse sign of three-body correlation functions. The differences in the present case are found to be negligible.

[9]P. Vogl, H. P. Hjalmarson, and J. D. Dow, J. Phys. Chem. Solids **44**, 365 (1983).

[10]W. I. Wang and F. Stern, J. Vac. Sci. Technol. B **3**, 1280 (1985).

[11]Some preliminary calculations were also performed using the slightly more realistic $Al_xGa_{1-x}As$ parameters of K. C. Hass, Phys. Rev. B **40**, 5780 (1989), and $\lambda = 0.6$. Good agreement was obtained for the Γ_1, L_1, X_1, and X_3 *band gaps* in the SQS-8 method (recursion method): 2.217 (2.215), 2.196

(2.185), 2.160 (2.145), and 2.640 (2.645) eV, respectively.

[12]The "GaAs" and "AlAs" entries in Table I differ from the crystalline eigenvalues of Ref. 9 because of the -0.47-eV shift of AlAs levels and the use of VCA parameters to describe the As on-site energies and nearest-neighbor hopping.

[13]Actually, one only need to consider those $T\mathbf{k}$ that are not related by operations of the SQS point group. In SQS-8, for example, only two ZB-structure X points are inequivalent.

[14]For $E_1 = -\infty$ and $E_2 = +\infty$, many of the lowest order M_p's associated with the present tight-binding Hamiltonian are easily evaluated analytically (following Ref. 1) and are found to be the same for the different techniques considered here at least up to $p = 5$. Over a more limited energy range, a strict equivalence no longer exists. Within our numerical accuracy, however, the computed $M_1(\mathbf{k})$ values in each approach are identical to those of the VCA.

[15]K. C. Hass, H. Ehrenreich, and B. Velický, Phys. Rev. B **27**, 1088 (1983).

[16]The predicted behavior for the X_3 state is exaggerated in Fig. 3 by the use of VCA off-diagonal parameters. Recursion calculations including off-diagonal disorder yield a single X_3 peak almost as sharp as that for X_1.

[17]The role of the X_3 state in producing an anomalous composition dependence of bowing of the direct band gap in $Al_xGa_{1-x}As$ has been discussed previously in S.-H. Wei and A. Zunger, Phys. Rev. B **39**, 3279 (1989). A similar effect is found in the tight-binding calculations of Ref. 18.

[18]L. C. Davis and K. C. Hass (unpublished).